

SRM Plume: a candidate as space debris braking system for Just-In-Time Collision Avoidance Maneuver

A. Jarry*, C. Dupont**, S. Missonnier**, L. Lequette**, C. Bonnal*, F. Masson*

* CNES, Launcher Directorate

52 rue Jacques Hillairet 75112 Paris, France

** Bertin Technologies, Expertise & Innovative Processes

25, route de l'Orme

Parc des Algorithmes, Bât. Esope 91190 Saint-Aubin, France

Abstract

A possible system suited for Just-In Time Collision Avoidance (JCA) is a cloud that will drag down the passing object because of the local higher density. The sudden deceleration experienced by the debris will after a few revolutions ensure a consistent deviation from its nominal trajectory and therefore will permit a safe reduction of any collision risk with other objects. This article first introduces a feasibility study of such a system, using as baseline an SRM and then enlarges the study to an enhanced system.

1. Introduction and requirements

1.1 Introduction

Since Sputnik-1 in 1957, the number and mass of orbital objects have continuously increased, reaching nowadays more than 18,600 catalogued objects and some 7,500 tons in orbit. This orbital population is composed of roughly 6% operational satellites, the rest being “artificial, non-functional, orbital objects”, i.e. orbital debris, which raises two concerns [9]:

- The first one is linked to the random atmospheric re-entry of large objects, in average more than once per week, with 10 to 20% of the mass surviving re-entry and potentially causing on-ground casualties; this topic is not addressed in this paper,
- The second one deals with the on-orbit collisions, in its vast definition.
 - The collision risks between catalogued and operational objects is dealt with through intensive “Collision avoidance” activities, inducing numerous maneuvers from every operator each year,
 - The situation in GEO is special, as there is no real risk of collision, but rather a problem of “freeing a parking lot”; the re-orbiting of defunct GEO satellite may turn out to be a significant market in the coming years,
 - Impacts from small untrackable debris, typically in the range of 5 to 100 mm, on operational satellites is a significant cause of satellite loss; simulations have shown that the probability of losing an active satellite over its nominal lifetime is today around 5%,
 - Collision between large non-maneuverable intact objects rarely occurs but results in generating a large number of new debris of various sizes at each occurrence, thus rapidly increasing the orbital population and consequently collision risks.

To counter the latter collisions among large intact objects, two approaches can be considered:

- The “strategic” one, as per the expression from Darren McKnight ([8]), consisting in the retrieval of a certain number of large debris each year, thus reducing the probabilities of major collisions. This Active Debris Removal (ADR) strategy has been intensively studied throughout the world for more than 10 years. It appears to be technically feasible, but hard to finance, and raises numerous non-technical problems such as legal or political ones. Furthermore, such ADR is useless as long as the internationally agreed mitigation rules are not correctly followed; indeed retrieving 5 large debris per year as identified in past references is of no use if we continue to leave in orbit more than 80 large debris deliberately (what has been done in 2016 for instance). There may be an exception in mid-future with the retrieval of defunct satellites from large-constellations for which a real business-plan may turn out to be profitable,

- The “tactical” one is aimed at avoiding an “announced” collision by acting on one of the two debris some time prior to the predicted collision. This strategy is called Just-in-time Collision Avoidance (JCA). The first ideas were presented some 10 years ago, and several studies are on-going now on this topic ([2] & [10]). Among the solutions which have been proposed, slightly slowing one of the debris thanks to the drag generated by an orbital gaseous cloud appears promising [11]. In the following chapters of this paper, we wish to describe a non-orbital system aiming at the same goal.

1.2 Context and high level requirements

Two large debris A and B are identified, having a probability of collision higher than a given threshold. Their orbits are determined, by JSpOC for instance, with a good precision several days before the potential collision, this information being refined over time thanks to dedicated radar measurements. Such a collision would generate thousands of new debris, so the decision to perform a JCA operation is decided by an ad-hoc international body (to be defined...).

A sounding rocket is launched from one of the dedicated bases in the world, aiming at deflecting one debris several orbits prior to the expected collision. These launch bases, typically 3 or 4, spread geographically, are located in zones such as to maximize the probability of being overflown by one of the two debris. Ideally, there should be a couple of these at high northern latitude, such as Kodiak Island, Kiruna, Andøya, Northern Russia...

The sounding rocket can be airborne, for instance under a heavy fighter aircraft, much in the way an Anti-Satellite demonstration was led against the satellite Solwind in September 1985, or launched from ground. It can be partially or totally reusable, with single or multiple stages.

On top of the upper stage is mounted a gas and particles generator, derived from a Solid Rocket Motor, with the nozzle aiming at anti-flight direction. This generator is fired while the sounding rocket is at culmination, close to the trajectory of the debris to be deflected and right before its transit time; the firing time and direction of the plume are adjusted such as to maximize the probability of an efficient interaction.

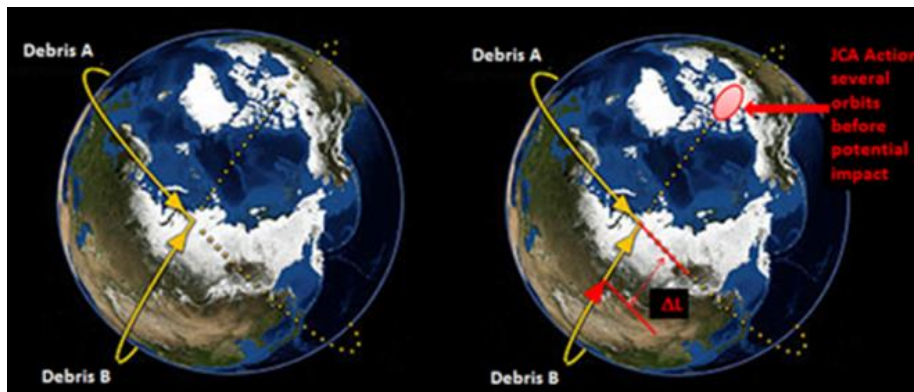


Figure 1: General principle of Just-in-time Collision Avoidance

The deflection δV imparted to the debris will slightly modify its semi major axis, thus its period by δT . Propagating this perturbation in time, one achieves the required miss distance ΔL . The relations between these variations are simple (Clohessy-Wiltshire equations):

$$\delta T = -3. T. \frac{\delta V}{V} \quad (1)$$

leading to

$$\Delta L = 3. \delta V. T \quad (2)$$

To give an order of magnitude of the corresponding requirements, one may consider the case schematized in Figure 1 with two debris at 800 km altitude. If one aims at generating a miss distance ΔL equal to 1 km, i.e. roughly 10 times the expected inaccuracy of orbital parameters with a JCA operation performed 24 hours before expected collision, then the required δV is equal to 3.8 mm/s. Of course, lowering the reaction time by a factor N increases the δV by this same factor N , and potentially raises a question on the availability of a suitable launch station to perform the operation. Same if one wishes to increase the miss distance by a factor N , the δV also increases by a factor N . For

instance, if the operation is performed 12 hours before the collision and one aims at 10 km miss distance, $\delta V = 76$ mm/s.

The principle of the studied system is depicted in Figure 2.

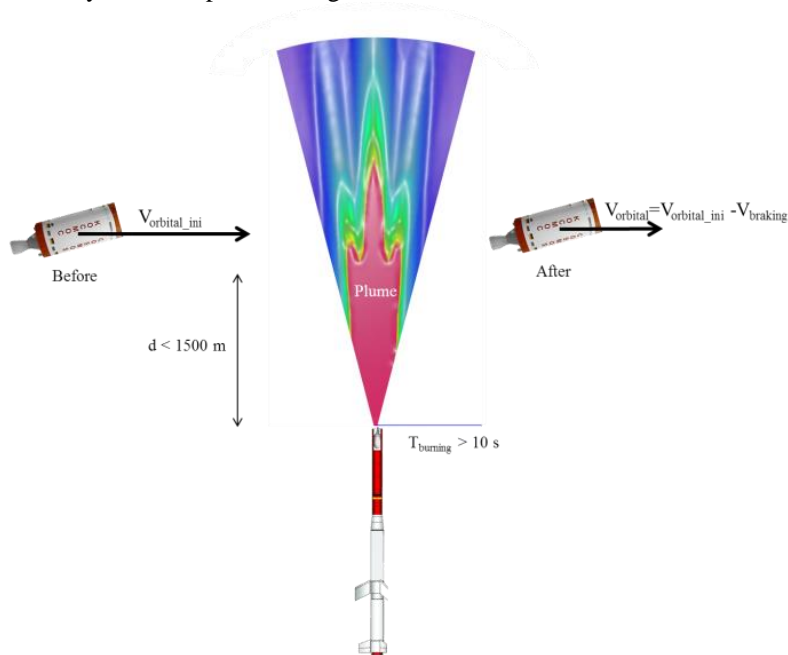


Figure 2: Schematic of the system studied

In the frame of this paper, the targeted ΔV is 1cm/s.

2. Computation Means

The objective of this study is to evaluate the braking capability of a cloud generated by a SRM. This requires both the computation of the SRM plume and the determination of the velocity decrease.

2.1 Brake capability computations

The debris is defined through the following parameters:

- Its mass M ;
- Its reference surface S ;
- Its drag coefficient C_x ;
- Its orbital speed v .

Moreover, the plume created by the SRM is characterized by

- Its local density ρ ;
- The relative speed v_r between the debris and the plume velocity.

On the debris' side, one assumes that the change of speed due to the cloud is negligible with respect to the orbital speed. Moreover, one supposes that the plume velocity is also negligible with respect to the orbital speed; this hypothesis is conservative, as it would increase the braking effect.

Using Newton's law, the debris acceleration can be expressed as

$$|\overline{Ma}| = |\overline{Drag}| = SC_x \frac{1}{2} \rho v_r^2 \quad (3)$$

Using the previous assumptions and

$$L = v\Delta t \quad (4)$$

one reaches the Δv via the formula:

$$\Delta v_{braking} = \frac{1}{M} S C_x \frac{1}{2} v \int_0^L \rho \delta x \quad (5)$$

The knowledge of the plume and the trajectory are thus the only information needed for the study.

2.2 Trajectory parameters

Any debris' trajectory with respect to the SRM can be characterized by three parameters as shown on Fig. 3:

- the parameter d is the distance in the orbital plane between the SRM and the trajectory of the debris,
- the parameter α is the angle in the orbital plane between the axis of the SRM and the trajectory of the debris;
- the parameter p is the out-of-plane deviation from the orbital plane (parallel to the SRM axis).

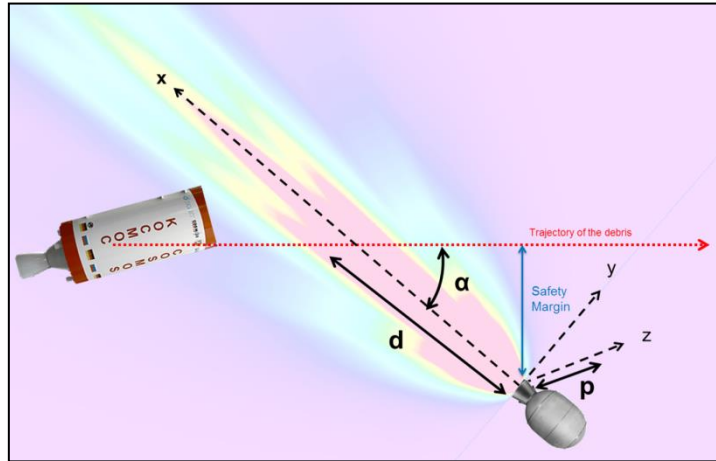


Figure 3: Definition of parameters of the trajectory

This set of parameters allows the definition of an envelope domain.

However, all trajectories are not deemed credible. For instance, having the same altitude for both SRM and object is not wished, nor it is desired a too small avoiding distance. The definition of allowed trajectories requires then an additional parameter that represents the safety margin, also depicted in Figure 3.

2.3 Plume computations

The plume modelling is performed using Bertin Technologies' homemade multiphysics code CPS_CTM. The solver is a diphasic Lagrangian solver and the computation is a steady one.

The phases are

- An equivalent gas corresponding to all the gaseous species;
- Alumina particles.

The computations take into account an interaction between gas and particles flow, such as drag and thermal exchanges. The alumina particles were modelled either using Hermesen model ([5] [6]) with a lognormal repartition evaluation or using a constant diameter assumption.

The mesh shown in Figure 4 is an axisymmetric one, with a 12-kilometers long extension on both axial and radial axes and a 5° angle.

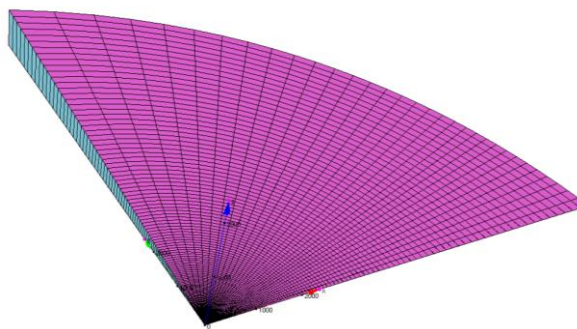


Figure 4: Computational mesh

A validation of the CFD simulation was performed by comparison to the plume of classical SRM from literature [7]. Figure 5 presents on the upper part a computation result of the mean particles diameter and on the lower part an experimental plume structure.

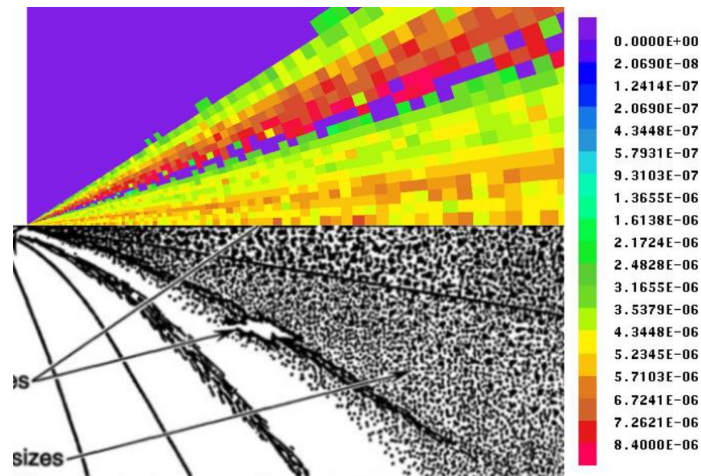


Figure 5: Comparison of SRM numerical and experimental ([7]) plume structure

The contours' plots highlight the existence of two different behaviors within the plume structure:

- The gas one with a propagation on the entire domain even with back-flow ;
- The particles one that is concentrated close to the axis.

As a matter of fact, alumina particles represent about 30% of the exhaust mass while their respective density is significantly higher than the equivalent gas one. Contrary to the gas, no expansion occurs to the particles in the nozzle's divergent part. Therefore, the trajectory of the particles remains in a restricted cone with respect to the gaseous field. Finally, because of the coupling gas-particles, the flow velocity is reduced close to the axis.

These features are highlighted in next figures (Fig. 6 showing the mean 2-phase flow density and Figure 7 introducing the particles density)

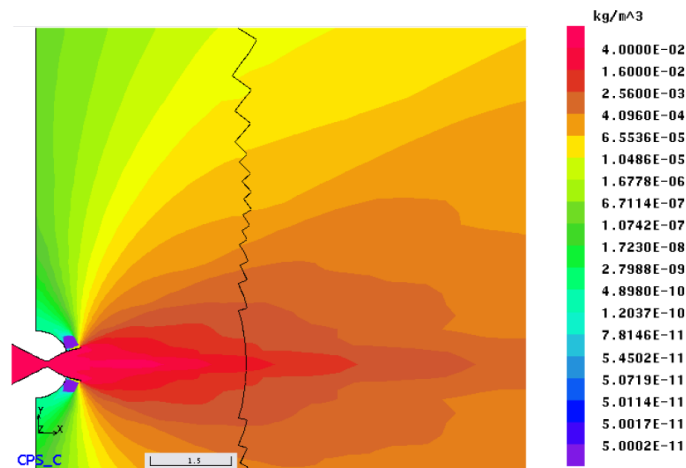


Figure 6: Two-phase flow density

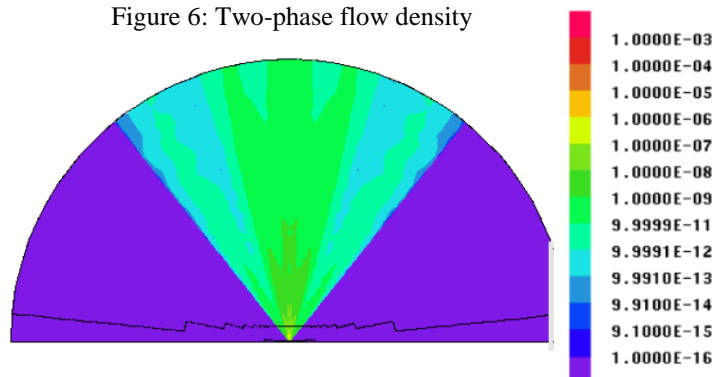


Figure 7: Particles density

The latter corresponds to a cone with an angle close to 35° . Within this zone, the particles are conveyed by the gas flow, the largest particles being limited in a restricted angle lower than 25° . Furthermore, the analysis of the gas velocity (Fig. 8) shows that the axial component is lower in the axis because of the alumina particles.

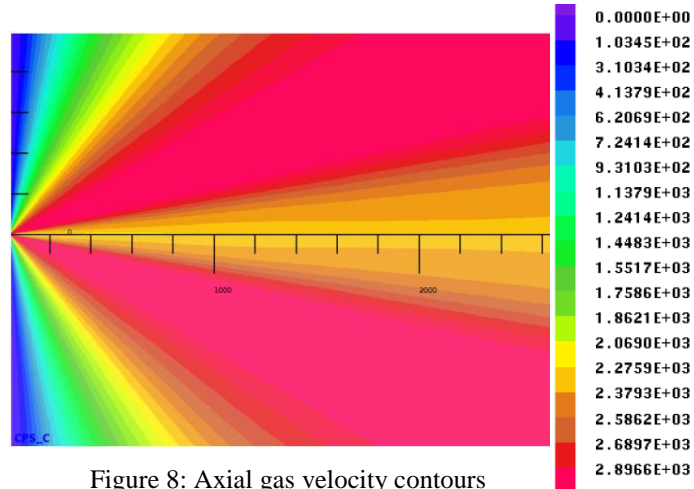


Figure 8: Axial gas velocity contours

Therefore, numerical results are coherent with experimental ones as well as observations made by other computations ([12], [13], [14], [15]). The plume modelling presented here is considered as representative for the study.

2.4 Computations objectives

The objective of this study is to find configurations that maximize the braking ΔV . The optimization problem consists in finding the trajectory that maximizes this ΔV . For each set of motor parameters, the problem can be formulated as follows:

$$\text{Maximize} \quad \Delta v_{braking}(z) \quad (6)$$

$$\text{With respect to} \quad z = \{d, \alpha, p\} \quad (7)$$

$$\text{Subject to} \quad g_1: \Delta v_{braking} > \Delta v_{braking_{min}} \quad (8)$$

$$g_2: d > d_{min} \quad (9)$$

3. Reference frame

3.1 Reference debris introduction

To calculate the $\Delta v_{braking}$, a reference debris has been considered: a COSMOS-3M (SL-8) orbital debris, shown in Figure 9.

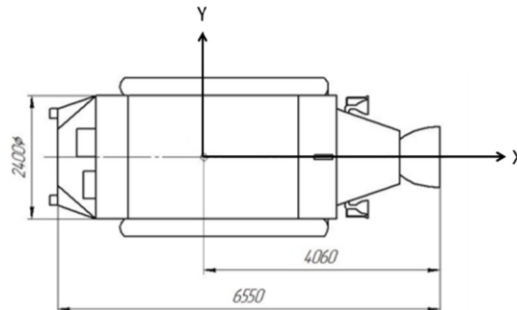


Figure 9: COSMOS geometry

The satellite is supposed to be rotating and the drag coefficient considers a mix of gas and particles. Indeed, the gas drag coefficient for high altitude is close to 2.5. For the particles, it is strongly dependent on their behavior (e.g. rebound, absorption). Therefore, a mean value of 1.73 was chosen.

Therefore, intrinsic characteristics taken for the debris are:

- Mass (M) : 1360 kg;
- S.Cx : 29.237 m² where S=16.9m²;
- Velocity (v): 7451.832 m/s (circular orbit at 800km).

3.2 SRM characteristics

The Star 48 Short Nozzle SRM is considered as baseline. Its characteristics are provided in [4] and it is shown in Figure 10.

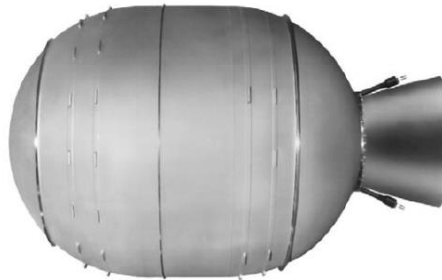


Figure 10: Star 48 Short Nozzle SRM [4]

The propellant is a HTPB 1811, the expansion ratio is 28.2 and the average total mass flow rate is 27.86 kg/s while the average pressure is 40 bar. One assumes a log-normal distribution of the particles ([5]).

4. Results

4.1 Reference case

The plume computation was performed thanks to CPS_C™ software.

The mean density contours (taking into account both particles and gas) are presented in Figure 11 on a 3-kilometer range.

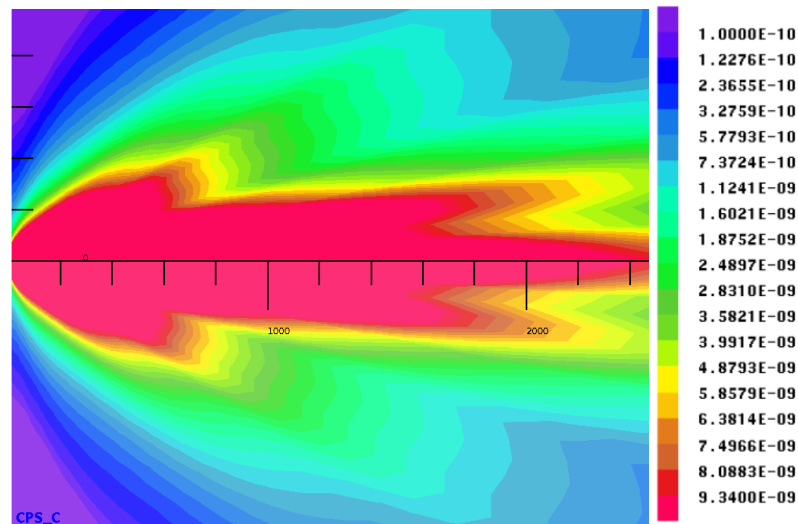
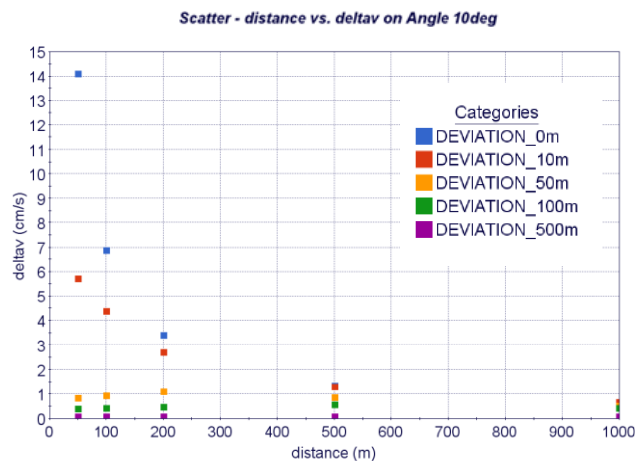
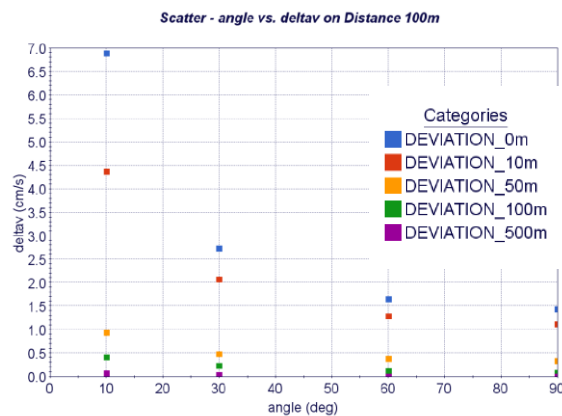


Figure 11: Plume of a SRM in vacuum space

Once the plume is computed, it is now possible to compute the braking possibility for various trajectories as well as to plot the results for two fixed parameters (e.g. Distance and deviation).

Figures 12 & 13 provide a first output with two parameters set, respectively the angle and the deviation in Figure 12, and the distance & deviation in Figure 13.

Figure 12: ΔV results with a 10° angleFigure 13: ΔV results with distance $d=100m$

This highlights the possibility to achieve the level of deceleration needed with a large number of parameters' sets. However, it is clear that the distance d and the deviation p are first order parameters:

- The lower the distance, the higher the ΔV .
- Furthermore, the possibilities' corridor associated to deviation p is even narrower since braking doesn't reach 1cm/s for deviation over 50m. .

After few hundred meters distance, the braking ΔV is too small to allow a sufficient braking of the debris. In consequence, the precision with respect to the orbital plane of the debris should be as high as possible.

Globally, the reference case features the plausibility of the SRM-based concept.

4.2 Sensitivities analyses

Given the capability of a SRM to fulfill the requirements for Just-In-Time Collision avoidance, it is of high interest to find ways to enhance the ΔV . Any upgrade of the ΔV will indeed allow widening the margins on the precision of the injection, i.e. relax operational constraints, as well as to decrease the mass of the system, i.e. improve its costs and operability.

Several options are analyzed:

- Influence of the alumina particles diameter;
- Variation of mean pressure and related mass fraction of alumina particles;
- Modification of the nozzle size (expansion ratio and length) and shape.

4.2.1 Particles diameter

As stated, the reference case is based on a log-normal distribution of particles size with a mean diameter close to 5 microns.

To assess the impact of the diameter, 6 different sets have been computed:

- 4 with constant diameter (1, 5.6 and 12 & 25 microns);

- 2 with log-normal distribution (and median diameter equal to either 5.6, or 12 microns).

Figure 14 exhibits two particles' distributions centered on the sizes aforementioned.

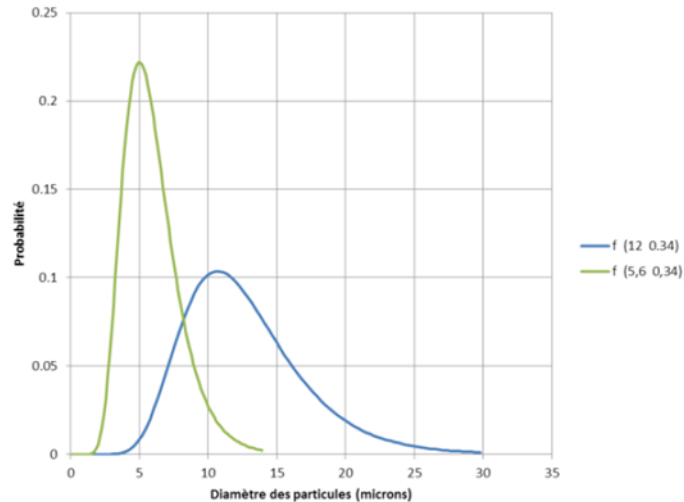


Figure 14: Examples of distribution of particles

A sample of results is given in Fig.15.

Two conclusions arise from this study:

- The lognormal distribution is a second order parameter with only a 10% gain from using a distribution rather than a constant value;
- The larger the particles, the larger the ΔV as expected. Furthermore, diameters higher than 5.6 μm produce ΔV in linear evolution;

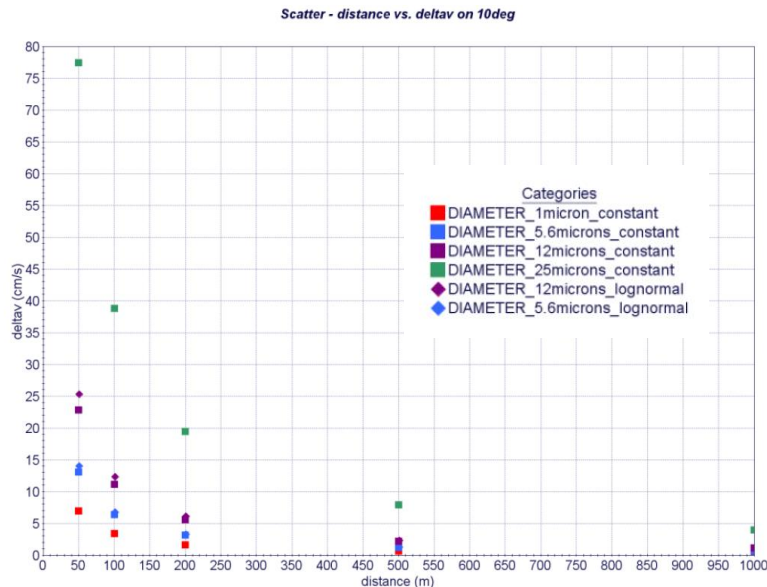


Figure 15: Impact of the particles' size and distribution on ΔV

4.2.2 Mass flow rate

It was decided to study in an independent manner the impact of a change in mass flow rate as well as the increase of the ratio (particles mass flow rate)/(total mass flow rate).

For the first item, chemical composition at the exit section is assumed to remain the same, independently of the chamber pressure. In terms of results, if the pressure drops by a factor of 2 (and consequently the mass flow rate), so does the computed ΔV .

For the second parameter, a diminution of the gas mass flow rate was applied while the particles mass flow rate stayed alike. This reduction corresponds to a lower chamber pressure.

The mean density contours are shown in the next figures. The lowering of the gas mass flow plays on the density contours, top left being the reference and the decrease in gas mass flow is represented clockwise. The blue lines represent the debris trajectory crossing the plume.

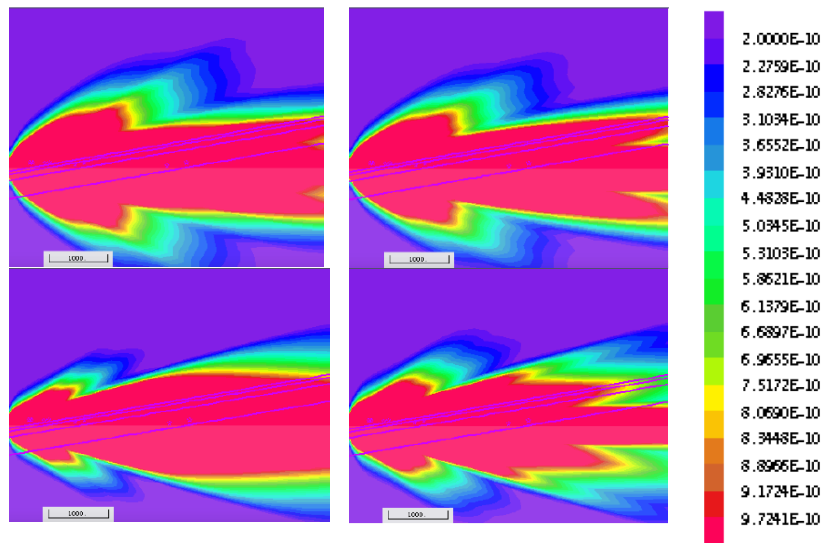


Figure 16: Impact of gas mass flow (corresponding to chamber pressure) on the plume density

The increase of mass fraction of alumina creates a high density cone starting from the nozzle. The gas is only used as a way to accelerate particles. However, the reduction of chamber pressure also induces a reduction of the particles' speed along with the diminution of the gas density. The results of the sensitivities are pictured in Figure 17.

Surprisingly, the higher the mass fraction of alumina particles, the higher the consequent ΔV . This is mainly due to the fact that particles are more concentrated within the axis and therefore mean diameter is higher with lower ejection speeds.

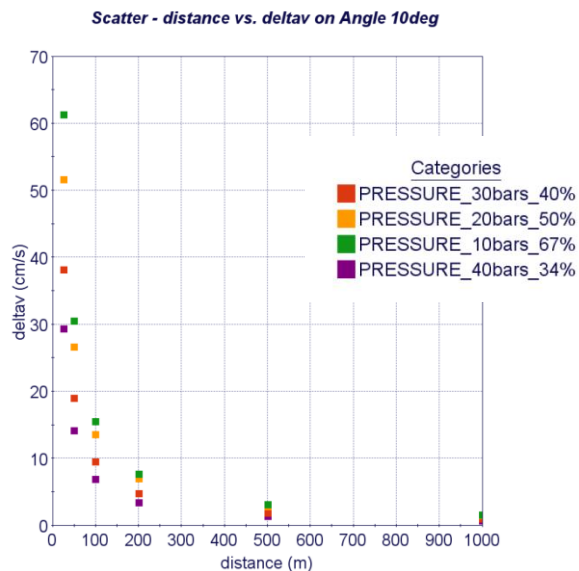
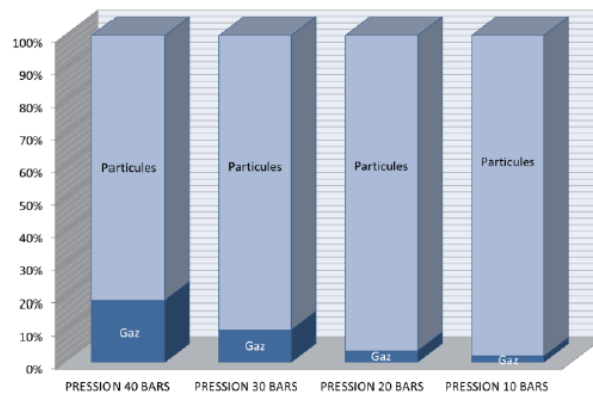


Figure 17: Impact of chamber pressure on the ΔV

An interesting feature of this sensitivity is the breakdown of gas and particles' contributions in the braking capacity. As a matter of fact, the contribution of particles is about 80% of the global number, as illustrated in the following picture.

Figure 18: Contribution of particles on ΔV

4.2.3 Nozzle evolution

The last sensibility that is performed is the influence of the nozzle's shape and main characteristics such as expansion ratio or length.

Several possible nozzles are shown in Fig. 19. A truncated cone, bell or conic shapes as well as different divergent angles have been looked at.

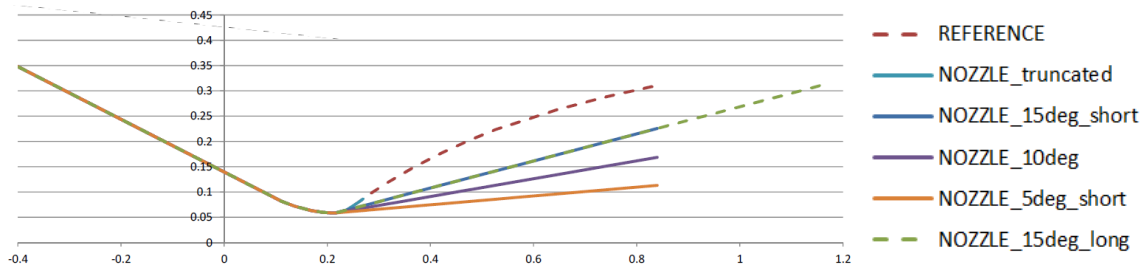
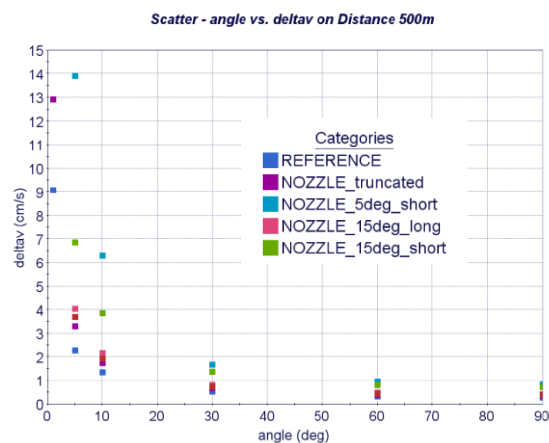


Figure 19: Nozzle configurations

This covers most of the possibilities offered in terms of nozzle morphing. The results showed in Figure 20 highlight the importance of these parameters on the braking.

Figure 20: Impact of the nozzle divergent on the ΔV

The main conclusions of the studies are:

- The bell-shaped nozzle configuration provides less ΔV than a conical nozzle one (with the same expansion ratio);
- The lower the cone angle, the higher the ΔV ;
- The nozzle truncated after the throat exhibits poor performance.

It is therefore of high interest to focus on configuration with low divergent angles. As a matter of fact, these angles aim at concentrating all gas and particles flow in a reduced cone.

4.2.4 Synthesis of sensitivities

The set of computations that was performed on some of the SRM parameters permits to evaluate the direction to follow so as to develop the most efficient system.

As a matter of fact, as shown in Fig. 21 for 10°-oriented trajectory, by combining all the best parameters together into a best case, the achieved ΔV can exceed 50 cm/s. This represents an increase of a factor of 14 with respect to the reference case (56 cm/s to be compared with less than 4 cm/s). The target of 1cm/s is overpassed by a 50 factor.

Surprisingly the increase of performance achieved with the best case is even better than the sum of all upgrades.

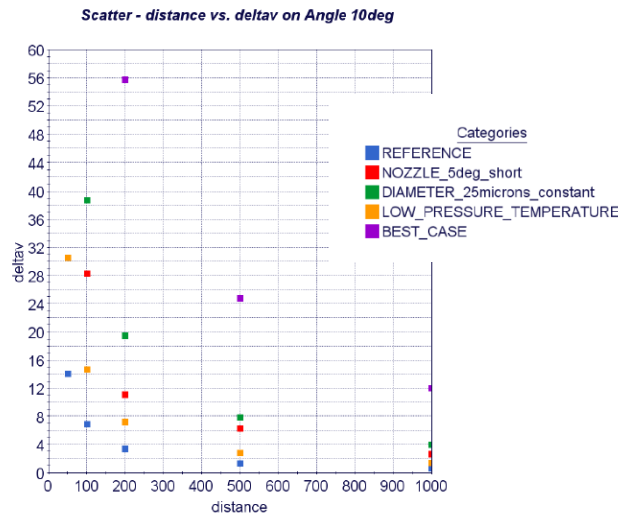


Figure 21: Impact of several ways of improvement of the ΔV

Through these circumvolutions, we can conclude that SRMs are suitable candidates for the task but not the most efficient ones. It appears that a gas & particles generator could better fit the job.

The targeted features of this generator are:

- low ejection speed;
- high diameter particles;
- short nozzle with a low angle.

5. Additional studies

5.1 Description

To complete the analysis and in order to seize a maximum efficiency by pushing all cursors towards the right direction, a new configuration was computed.

It is based on:

- a N_2 pressurized tank at 298 K with a 100 bar inner pressure at $t=0s$;
- Copper particles with a 50 μm diameter;
- A throat of 11.6 cm;
- A short nozzle with 5° angle;

The ground behind the temperature choice is the need to reduce the gas exit velocity while the copper particles diameter is a grade available for sale.

5.2 Assumptions and performance target

One considers that the particles mass flow is the same as the STAR one.

Small adjustments on the debris' definition were also performed:

- $S_{ref}=14.47m^2$ (previously 16.9 m^2)
- $C_x = 1.7$ (previously 1.73)

Finally, one considers the following fixed parameters for the debris trajectory:

- Distance $d=100m$;
- Angle 45°;

- Deviation close to 0m.

5.3 Results

Three cases were computed:

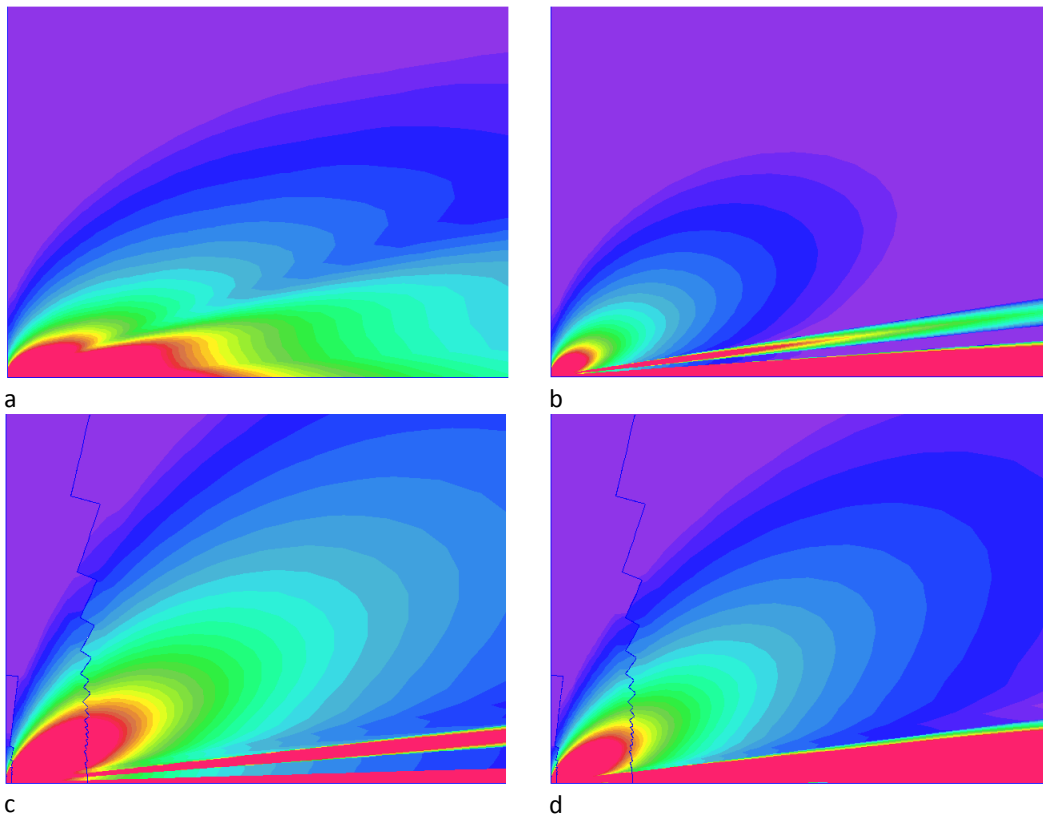
- Case 1 (“New solution – case 1”) corresponds to $t=2s$ after the opening of the tank valve;
- Case 2 corresponds to $t=4s$ after the opening of the tank valve, therefore with a lower mass flow rate;
- Case 3 corresponds to case 1 with a change of nozzle towards the Star 48 one.

The following table describes the considered input conditions.

Table 1: Computations’ cases

	Gas mass flow rate	Total pressure [bar]	Total temperature [K]	Nozzle
SRM solution (a)	9.2	40	3556	Star 48 short nozzle
Best case with SRM (b)	9.2	20	3556	5°
New solution – case 1 (c)	9	7.3	266	5°
New solution – case 2 (d)	7	2.5	228	5°
New solution – case 3 (e)	9	7.3	266	Star 48 short nozzle

The following figures show the contours in terms of mean density starting from the SRM solution (a), then the other solutions from b to e.



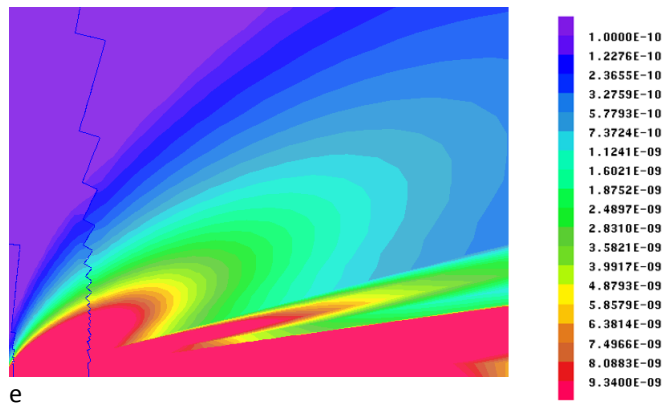


Figure 22: Contours of mean density for various computations' cases

The influence of the tank pressure can be clearly seen for the gas part as well as the influence of the nozzle shape. The computation of the braking capability was then performed for the 5 configurations on the dedicated trajectory set.

Results are given in Table 2 along with 3 other trajectory sets.

Table 2: Results

	ΔV [cm/s] $\alpha=45^\circ$ d=100m p=0.2m	ΔV [cm/s] $\alpha=45^\circ$ d=1000m p=0.2m	ΔV [cm/s] $\alpha=90^\circ$ d=100m p=0.2m	ΔV [cm/s] $\alpha=45^\circ$ d=100m p=50m
SRM solution (a)	1.2	0.1	0.8	0.32
Best case with SRM (b)	20	1.9	13.7	0.12
New solution – case 1 (c)	177	18	125	1.06
New solution – case 2 (d)	70	[5.5-8]	[40-60]	0.5
New solution – case 3 (e)	15	1.4	10.5	1.26

The table highlights the extraordinary capability of this system to fulfill the job with high margins as long as deviation is close to 0. These margins allow envisaging an altered precision for the distance to the debris or deviation of the orbital plane since even with 1 kilometer distance, this N₂ and copper system achieves about 500 times the required value of 3.8 mm/s. As a matter of fact, even with a 50m deviation, the new solutions satisfy the requirements.

These values were established considering a Cosmos 3M (SL-8) upper stage, but they can easily be extrapolated to any other larger intact debris; for instance, considering a Zenit upper stage (SL-16) would reduce the results by a factor 2.28.

6. Conclusions

A new concept of JCA, aiming at slightly deviating a debris in order to prevent a collision, derived from a Solid Rocket Motor used as a particles generator, is proposed.

The preliminary feasibility study presented here has shown unexpected good results, orders of magnitude better than the strict requirement. These studies have shown that the optimal concept consists in a system releasing solid particles at low velocity, with a relatively tight plume shape correctly optimized.

As risks reduction approach and because of the reduced margins, sensibilities have also been assessed. They bear upon particles size & flow rate as well as nozzle shape and dimensions. These analyses revealed directions to be followed to foster the increase of braking ΔV . They have globally shown a good robustness of the concept. However, obviously, this is only the very first step of the feasibility study. One has now to perform the system study, consolidating (or not) the values of the key parameters considered here, as the distance between the SRM and the debris, or the out-of-plane mismatch distance. One has also to assess the global feasibility of the mission, taking into account the launch of the sounding rocket, deviations of its trajectory, homing... It may still very well turn out as being impossible, but so far, so good!

Acknowledgement

This study was performed by Bertin Technologies under CNES contract.

References

- [1] J.-C. Liou, *Engineering and Technology Challenges for Active Debris Removal*, 4th European Conference for Aerospace Sciences (EUCASS), 2011.
- [2] Dr. Darren S. McKnight, *Engineering and Operational Issues Related to Just-In-Time Collision Avoidance (JCA)*, 6th European Conference for Aerospace Sciences (EUCASS), 2015.
- [3] D.S. McKnight, F. Di Pentino, K. Walbert, S. Douglass, *Developing a Tactical Adjunct to Insure a Sustainable Space Environment*, IAC-15,A6,2.7x28443, 66th International Astronautical Congress, Jerusalem, 2015.
- [4] ATK Space Propulsion Product Catalog, 2008
- [5] R.W. Hermsen, *Aluminium oxide particle size for solid rocket motor performance*, AIAA 19th aerospace science meeting, AIAA-81-0035, January 12-15, 1981.
- [6] J.K. Sambamurthi, *Plume Particle Collection, and Sizing from Static Firing of Solid Rocket Motors*, AIAA 95-290, 31st Joint propulsion conference and exhibit, July 10-12, 1995, San Diego, CA.
- [7] F.S. Simmons, *Rocket Exhaust Plume Phenomenology*, ISBN 1-884989-08-X , Aerospace Corporation, 2000.
- [8] D. Mc Knight, Ch. Bonnal, *Operations for generating reliable encounter mass clouds for Just-in-time Collision Avoidance*, Proceedings from 4th International Workshop on Space Debris Modeling and Remediation, Paris, 6-8 June 2016
- [9] IAA Situation Report on Space Debris – 2016, <http://iaaweb.org/content/view/487/655/>
- [10] C. Phipps, Ch. Bonnal, *A spaceborne, pulsed UV laser system for re-entering or nudging LEO debris, and re-orbiting GEO debris*, ActaAstronautica18(2016)224–236
- [11] Levit, NASA Ames ADR efforts, *Proceedings of the International Conference on Orbital Debris Removal*, Chantilly, USA, December 8-10, 2009
- [12] J.M. Burt, I.D. Boyd, *Monte-Carlo Simulation of particles Radiation in high Altitude solid Rocket plumes*, 43rd AIAA/ASME/SAE/ASEE Joint Propulsion Conference & Exhibit, 2007, Cincinnati, Ohio
- [13] Agard Advisory Report 287, *Propulsion and Energetics Panel working group 21 on Terminology and assessment methods of Solid propellant Rocket Exhaust Signatures*, February 2013
- [14] J. Troyes, I. Dubois, V. Borie, A. Boischot, *Multi-phase reactive numerical simulations of a model solid rocket motor exhaust jet*, 42nd AIAA/ASME/SAE/ASEE Joint Propulsion Conference & Exhibit, 2006, Sacramento, California
- [15] A. Poubeau, *Simulation des émissions d'un moteur à propergol solide : vers une modélisation multi-échelle de l'impact atmosphérique des lanceurs*, Rapport de thèse, 2015